

# Electronic Structures and Applications of Carbon Nanotubes

Philip Kim, Teri W. Odom, Jinlin Huang, and Charles M. Lieber

*Harvard University, Cambridge, MA 02138, USA*

**Abstract.** The electronic density of states (DOS) of atomically resolved single-walled carbon nanotubes have been investigated using scanning tunneling microscopy. Peaks in the DOS due to the one-dimensional (1D) nanotube band structure have been characterized and compared with the results of tight-binding calculations. In addition, a novel electromechanical device has been designed and fabricated using nanotubes.

## INTRODUCTION

There has been intense effort focused on carbon nanotubes since their discovery by Iijima [1]. This attention on carbon nanotubes is not surprising in light of their promise to exhibit unique physical properties that could impact broad areas of science and technology, ranging from super strong composites to nanoelectronics [2]. According to theory [3], SWNTs can exhibit either metallic or semiconducting behavior depending on diameter and helicity. Recent scanning tunneling microscopy (STM) experiments [4,5] have resolved the atomic structure and electronic density of states of SWNTs, and have confirmed this predicted electronic behavior of SWNTs. In addition, the tunneling spectra reported in these studies exhibited peaks in the density of states (DOS), Van Hove singularities (VHS), that are believed to reflect the 1D band structure of the SWNT [6].

In this paper, we first review STM investigations of the electronic structure of atomically resolved SWNTs and compare these results with tight-binding calculations. Significantly, we find that the VHS in the DOS calculated using a straightforward zone-folding approach agree with the major features observed in the spectroscopic measurements. In addition, we will also discuss the design and fabrication of an electromechanical device that exploit these unique electrical and mechanical properties of nanotubes.

CP486, *Electronic Properties of Novel Materials— Science and Technology of Molecular Nanostructures*, edited by H. Kuzmany, J. Fink, M. Mehring, and S. Roth

© 1999 American Institute of Physics 1-56396-900-9/99/\$15.00

## VAN HOVE SINGULARITIES IN SINGLE-WALLED NANOTUBES

SWNT samples were prepared by laser vaporization, purified and then deposited onto a Au (111)/mica substrate. Immediately after deposition, the sample was loaded into a UHV STM that was stabilized at 77 K; all of the experimental data reported in this paper were recorded at 77 K. Imaging and spectroscopy studies were carried out using etched tungsten tips with the bias ( $V$ ) applied to the tip. STM spectroscopy measurements were made by recording and averaging 5 to 10 tunneling current ( $I$ ) versus  $V$  ( $I$ - $V$ ) curves at specific locations on atomically resolved SWNTs. The tunneling conductance,  $dI/dV$ , was obtained by numerical differentiation.

An atomically resolved STM image of several SWNTs is shown in Fig. 1(a). The diameter and chiral angle measured for this tube were  $1.35 \pm 0.1$  nm and  $-20 \pm 1^\circ$ , respectively after deconvolution of tip effects [7]. The measured diameter and chiral angle can be used to assign the  $(n, m)$  indices of the SWNT [4,7]. We find that (13, 7) and (14, 7) are consistent with the uncertainty in these values, where (13, 7) and (14, 7) are expected to be metallic and semiconducting respectively. The  $I$ - $V$  exhibits metallic behavior with relatively sharp, stepwise increases at larger  $|V|$  (Fig. 1(b)). The  $I$ - $V$  curves have a finite slope, and thus the normalized conductance  $(V/I)(dI/dV)$ , which is proportional to the LDOS, has appreciable non-zero value at  $V = 0$  as expected for a metal (Fig. 1(b) inset). This suggests that the (13, 7) indices are the best description of the tube (we address this point further below). At larger  $|V|$ , several sharp peaks are clearly seen in both the  $dI/dV$  and the normalized conductance. We attribute these peaks to the VHS

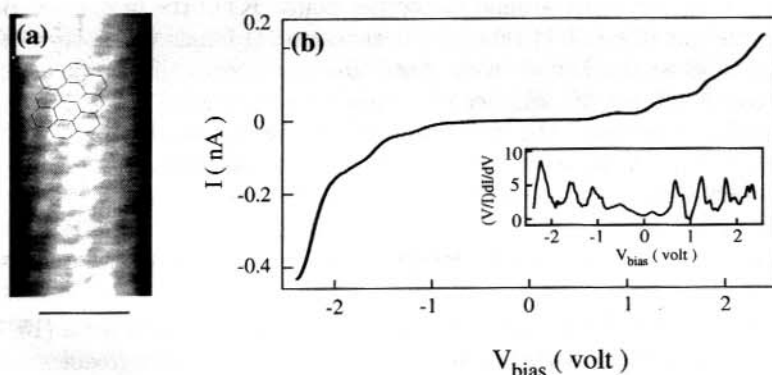


**FIGURE 1.** (a) STM image of SWNTs recorded at  $I = 0.12$  nA and  $V = 550$  mV. The black scale bar is 1 nm. A portion of a hexagonal lattice is overlaid to guide the eye. (b)  $I$ - $V$  data recorded on the SWNT in (a). The inset shows the normalized conductance,  $(V/I)(dI/dV)$ . (adapted from [6]).

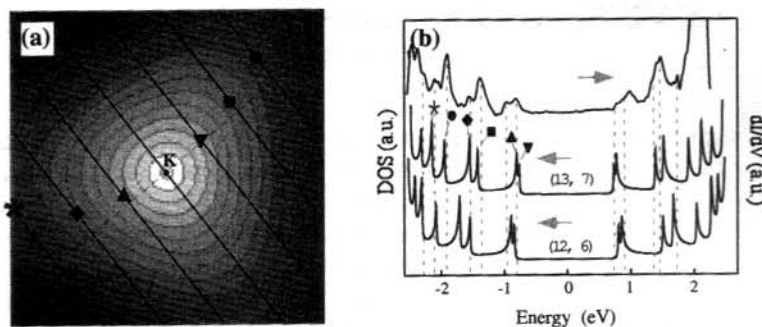


**FIGURE 2.** (a) Energy dispersion of the  $\pi$ -band of graphene sheet near  $\mathbf{K}$ . The solid lines correspond to  $(13, 7)$  1D bands obtained by the zone-folding. Symbols are located at the positions where VHS occur in these 1D bands. (b) Comparison of DOS obtained from our experiment (upper curve) and  $\pi$ -only tight binding calculation for  $(13, 7)$  and  $(12, 6)$  SWNT (the second curve from top). The broken vertical lines indicate the positions of VHS in the tunneling spectra after considering convolutions of thermal broadening. The symbols correspond to the VHS shown in (a) (adapted from [6]).

resulting from the extremal points in the 1D energy bands.

The availability of experimentally determined density of states for atomically-resolved nanotubes represent a unique opportunity for comparison with theory. In this regard, we have calculated the band structure of a  $(13, 7)$  SWNT using the tight-binding method. If only  $\pi$  and  $\pi^*$  orbitals are considered, the SWNT band structure can be constructed by zone-folding the 2D graphene band structure into the 1D Brillouin zone specified by the  $(n, m)$  indices [2]. Fig. 2(a) shows the graphene  $\pi$  band structure around the corner point ( $\mathbf{K}$ ) of the hexagonal Brillouin zone. For the metallic  $(13, 7)$  tube, the degenerate 1D bands which cross  $\mathbf{K}$  result in a finite DOS at the Fermi level. Note that the energy dispersion is isotropic (circular contours) near  $\mathbf{K}$ , and becomes anisotropic (rounded triangular contours) away from  $\mathbf{K}$ . Therefore, the first two VHS in the 1D bands closest to  $\mathbf{K}$  have a smaller splitting in the energy due to the small anisotropy around  $\mathbf{K}$ , while the next two VHS have a larger splitting due to increasing anisotropy. If the energy dispersion were completely isotropic, both sets of peaks would be degenerate. We used the same value of the hopping integral  $V_{pp\pi}$ , 2.5 eV, determined from previous studies [4,7].

Our STS data shows relatively good agreement with the DOS for a  $(13, 7)$  tube calculated using the zone-folding approach (Fig. 2(b)). The agreement between the VHS positions determined from our  $dI/dV$  data and calculations are especially good below the Fermi energy ( $E_F$ ) where the first seven peaks correspond well. Above the Fermi energy larger deviations between experiment data and calculations exist. The observed differences may be due to the band repulsion, which arises from the curvature-induced hybridization, or surface-tube interaction that

were not accounted for in our calculations. Detailed *ab initio* calculation [8] have shown that the effect of curvature induced by hybridization is greater in  $\pi^*/\sigma^*$  than  $\pi/\sigma$  orbitals. This could explain the greater deviations between experiment and calculation that we observe for the empty states. In the future, we believe that comparison between experiment and more detailed calculations will help to resolve such subtle but important points, and also help to understand how inter-tube and tube-substrate interactions affect the nanotube band structure. We have also investigated the sensitivity of the DOS to  $(n, m)$  indices. Specifically, we calculated the DOS of the next closest metallic SWNT to our experimental diameter and angle, a (12, 6) tube. Significantly, we find that the calculated VHS for this (12, 6) tube deviate much more from the experimental DOS peaks than in the case of the (13, 7) tube (Fig. 2(b)). We believe that this analysis not only substantiates our assignment of the indices in Fig. 1(a), but more importantly, demonstrates the sensitivity of detailed DOS to subtle variations in diameter and chirality.

## ELECTROMECHANICAL DEVICES USING NANOTUBE: NANOTWEEZER

Carbon nanotubes are both electrically conducting and mechanically flexible, and thus offer many unique opportunities for creating nanoscale devices. In this section, we will discuss the design and fabrication of an electromechanical nanotube device, a nanotweezer.

A nanotweezer was fabricated in two basic steps. First, two independent, electrically isolated gold electrodes were deposited on the surface of a micro-pipette by shadow masking during thermal deposition. Second, multi-walled nanotubes were attached to each electrode, and firmly fixed by conducting carbon polymer tape [9,10].

The operation of the nanotweezer was investigated by applying a bias voltage to the electrodes. The mechanical deflection of tweezer arms was observed in an inverted optical microscope, and recorded using a CCD camera and frame grabber attached to the microscope. Figure 3 shows the voltage response of a typical nanotweezer. As the bias voltage increases from 0 V to 20 V, the end of tweezer arms gradually close, and then touch. It was found that the tweezer arms relaxed to the original position when the applied bias voltage was removed, and this process can be done several times producing the same deflection. This verifies that the deflection of tweezer arms is mainly attributed to elastic deformation of the nanotubes rather than plastic deformation between nanotubes and metal electrodes. Therefore, the device demonstrates repeatable tweezer operation, and moreover the bias voltage required for actuation is considerably lower than that was required for the previous microtweezer [11].

Once the tweezer arms are closed tightly ( $\sim 20$  V in Figure 3), they remain stuck together even after removing the applied bias voltage. The strong adhesion force between bundles of multi-walled nanotubes are presumably responsible for

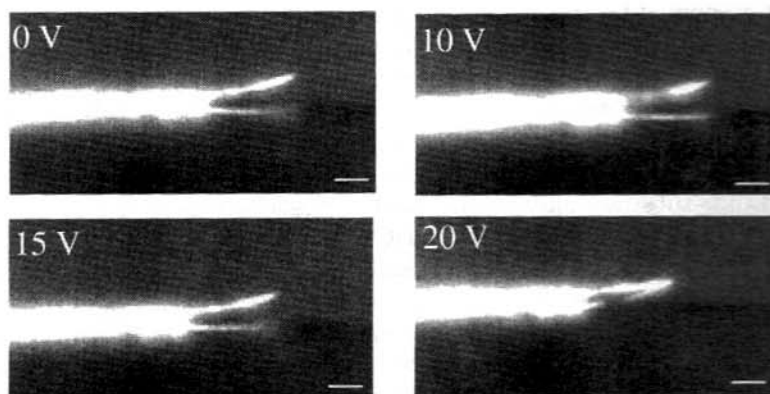


**FIGURE 3.** Mechanical deflection of nanotweezer in the response to bias voltages.

this observed behavior. The closed end of the tweezers, however, could reopen by applying the same polarity of voltage to both sides of the tweezer arms to charge the ends.

## SUMMARY

We have discussed STM investigations of the electronic structure of atomically resolved SWNTs and compared these results with tight-binding calculations. Significantly, we find good agreement between the major features observed in the spectroscopic measurements and the VHS predicted by tight binding calculations. In addition, the unique properties of nanotubes were exploited to fabricate an electromechanical nanotweezer.

## REFERENCES

1. S. Iijima, *Nature* **354**, 56 (1991).
2. M. S. Dresselhaus *et al.*, *Science of Fullerenes and Carbon Nanotubes* (Academic, San Diego, 1996).
3. J. W. Mintmire *et al.*, *Phys. Rev. Lett.* **68**, 631 (1992); N. Hamada, *et al.*, *Phys. Rev. Lett.* **68**, 1579 (1992); R. Saito *et al.*, *Appl. Phys. Lett.* **60**, 2204 (1992).
4. T. W. Odom *et al.*, *Nature* **391**, 62 (1998).
5. J. W. G. Wildoer *et al.*, *Nature* **391**, 59 (1998).
6. P. Kim *et al.*, *Phys. Rev. Lett.* **82**, 1225 (1999).
7. T. W. Odom *et al.*, *J. Mater. Res.* **13**, 2380 (1998).
8. X. Blase *et al.*, *Phys. Rev. Lett.* **72**, 1878 (1994).
9. H. Dai *et al.*, *Nature (London)* **384**, 147 (1996).
10. S. S. Wong *et al.*, *Nature (London)* **394**, 52 (1998).
11. N. C. Macdonald *et al.*, *Sensors and Actuators* **20**, 123 (1989).